Structures and Bonding of Early Transition Metallaborane Clusters

Stutee Mohapatra, Sourav Gayen, Ranjit Bag, A Das, Rongala Ramalakshmi, Marie Cordier, Sundargopal Ghosh

Structures and Bonding of Early Transition Metallaborane Clusters

Stutee Mohapatra,† Sourav Gayen,† Ranjit Bag,† Arpita Das,† Rongala Ramalakshmi,† Marie Cordier#, and Sundargopal Ghosh*,†

† Department of Chemistry, Indian Institute of Technology Madras, Chennai 600036, India. Tel: +91 44-22574230; Fax: +91 44-22574202; E-mail: sghosh@iitm.ac.in

Univ Rennes, CNRS, Institut des Sciences Chimiques de Rennes, UMR 6226, F-35000 Rennes, France

ABSTRACT: Structures and bonding of various homo and heterometallic metallaborane clusters are described which are stabilized in the coordination sphere of early transition metals. For example, the bimetallic triborane species, [{Cp*Mo(CO)}$_2${μ-η^3:η^3-B_3H_7}], **2** has been synthesized from the pyrolysis of an *in situ* generated intermediate, produced from the reaction of [Cp*Mo(CO)$_3$Me], **1** and [LiBH$_4$·THF], with an excess amount of [BH$_3$·THF]. Superficially cluster **2** is isostructural but not isoelectronic with [(Cp*MoCl)$_2$B$_3$H$_7$] (**I**). Both clusters **2** and **I** contain a bimetallic template bridged by {B$_3$H$_7$} moiety. Cluster **2** is denoted as a unique saturated and unsubstituted *closo* bimetallic B$_3$H$_7$ cluster. Theoretical output implies that saturation in such clusters brings thermodynamic stability. Further, we have developed a new strategy for the synthesis of various heterometallic metal-rich metallaborane clusters. For example, pyrolysis of an intermediate, obtained from the reaction of [Cp*MoCl$_4$], **4** and [LiBH$_4$·THF], with cobalt and iron carbonyl compounds yielded triply bridging hydrido(hydroborylene), [{Cp*Mo(CO)$_2$}$_2$Co(CO)$_3$BH(μ-H)], **5**, tetrametallic μ_4-boride, [{Cp*Mo(CO)$_2$}$_2$(μ_4-B)(μ-H){Co$_2$(CO)$_5$}], **6,** triple decker complex, [(Cp*Mo)$_2${μ-η^6:η^6-B$_4$H$_4$Co$_2$(CO)$_5$}(μ-H)$_2$], **7**, metal-rich dimolybdaborane cluster, [(Cp*Mo)$_2$Co$_2$(CO)$_3$(μ-CO)$_3$B$_3$H$_3$(μ-H)$_2$], **8** and mixed-metal cluster, [(Cp*Mo)$_2$B$_4$H$_8$Fe(CO)$_3$], **9**. All the molecules have been characterized by ^{1}H, ^{11}B{^{1}H}, and ^{13}C{^{1}H} NMR spectroscopy; mass spectrometry; infrared (IR) spectroscopy and single-crystal X-ray diffraction studies for clusters **2** and **5**-**9**. The electron counting rules and density functional theory (DFT) calculations provided further insight into the bonding and electronic structures of these clusters.

INTRODUCTION

Due to the unique nature of bonding, the lower borane species have been utilized outwardly in many organic syntheses, for example, catalytic diboration, hydroboration and borylation reactions.[1] However, the right-hand neighbours of boron show different properties and one of them is catenation property that led to the formation of consecutive C-C bonds or Si-Si bonds in chemistry of polysilanes. In contrast, due to the electron deficiency, boron favors to oligomerize through non-classical three centered two electron bonding instead of classical electron precise two centered two electron bond unless stabilized by electron donating substituents.[2] For example, as shown in Chart 1[3-7], linear catenated triborane(5), **A**[3] has been stabilized by bulky diamino substituents on terminal boron atom. However, with increasing number of boron atoms, they lean towards cluster formation, in which the triborane or tetraborane typically prefer cyclic form[8]. Interestingly, Braunschweig *et al.* reported the hydroboration of diborenes that generated unique bis(NHC)-stabilized triborane **B**.[4a] Successively they have synthesized electron precise sp^3-sp^2-sp^3 triborane **C** from ferrocene-bridged diborene.[4b]

Chart 1. Various types of triborane species (A-F). M= Pd or Pt, E =SePh.

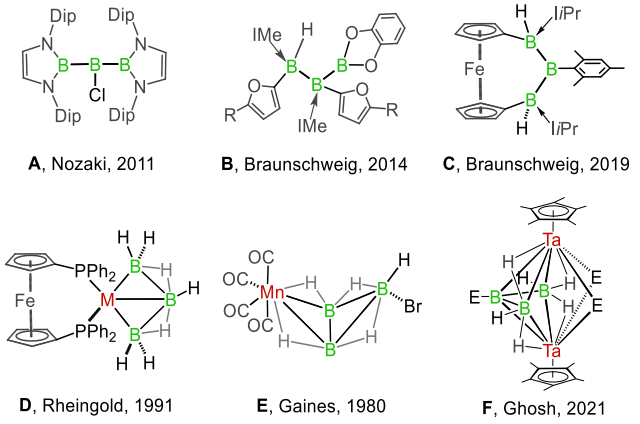

The triborane moiety is the simplest polyborane in which distinct bonding modes with metal counterparts have been observed.[9] Triborane **D**,[5] shown in Chart 1, represents a π-borallyl triborane ligand, which is coordinated to metal with pseudo square-planar environment. In 1980, Gaines and coworkers isolated and structurally characterized a fascinating butterfly cluster [(CO)$_4$MnB$_3$H$_8$Br],[6] **E**, in which the bidentate B$_3$ ring is ligated to Mn(CO)$_4$ moiety. To the best of our knowledge, the numbers of linear triboranes are very limited except some structurally characterized B$_3$H$_8$-metal clusters. To isolate such kind of species, transition metal coordination sphere is considered to be one of the key

templates that can stabilize the unstable reactive motifs.[7,10] For example, recently we have isolated a classical $[B_2H_5]^-$ ion stabilized by binuclear tantalum template.[10a] Subsequently, we have isolated a triborane analogue $\{B_3H_6SePh\}$ which is also stabilized in the coordination sphere of $\{Cp^*Ta\}_2$.[7] Further, a bimetallic diborane(4) species, $[\{Cp^*Mo(CO)_2\}_2\{\mu\text{-}\eta^2\text{:}\eta^2\text{-}B_2H_4\}]$[10b] was isolated which is stabilized by $\{Cp^*Mo\}_2$ fragment. Note that isolobal analogy[11] and electron counting[12] rules play a major role in designing and synthesizing these species, which are stabilized by early transition metal template.

Therefore, with an objective to isolate such metal coordinated lower borane species, we explored the reaction of an in situ generated intermediate, made from the reaction of $[Cp^*Mo(CO)_3Me]$ and $[LiBH_4{\cdot}THF]$, with an excess of $[BH_3{\cdot}THF]$. The reaction yielded linear triborane species, confined in metal templates. In this article, we described the details of their structure, bonding and spectroscopic characterization. In addition, we have further explored the reactivity of $Co_2(CO)_8$ and $Fe_2(CO)_9$ with another in situ generated intermediate, generated from the reaction of $[Cp^*MoCl_4]$ and $[LiBH_4{\cdot}THF]$, that yielded novel metal-rich metallaborane clusters.

RESULTS AND DISCUSSION

Low temperature reaction of $[Cp^*Mo(CO)_3Me]$, **1**, with $[LiBH_4{\cdot}THF]$ followed by mild pyrolysis with $[BH_3{\cdot}THF]$ resulted in the formation of an air and moisture sensitive green solid **2** (Scheme 1). The reaction also yielded *arachno*-$[Cp^*Mo(CO)_2B_3H_8]$[10c], **3** and $[(Cp^*Mo)_2B_5H_9]$ along with other unstable as well as moisture sensitive compounds, which we were unsuccessful in isolating in pure form. Compound **2** was characterized by ^1H, ^{11}B, ^{13}C NMR, IR, mass spectrometry and single crystal X-ray diffraction study. The $^{11}B\{^1H\}$ NMR spectrum of **2** shows two resonances at δ = 12.9 and -3.7 ppm ~2:1 ratio. Alongside peaks at δ = 3.01 ppm and 1.57 ppm for the B-H terminal protons, the ^1H NMR spectrum shows two distinct Cp* proton peaks at δ = 2.02 and 1.90 ppm. Additionally, a broad up-field resonance at δ = -13.08 ppm has been detected. The IR spectrum of **2** featured bands at 1638 and 2475 cm^{-1} corresponding to carbonyl and terminal B-H ligands, respectively. Later, the $^{13}C\{^1H\}$ NMR spectrum of **2** also suggests the existence of

Scheme 1. Synthesis of $[\{Cp^*Mo(CO)\}_2\{\mu\text{-}\eta^3\text{:}\eta^3\text{-}B_3H_7\}]$ (Mo-Mo bonds are not shown for clearness).

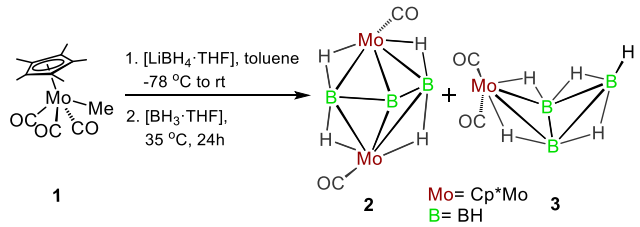

Cp* and CO ligands. The mass spectrum of **2** shows the parent ion peak at *m/z* 558.1215 that corresponds to $[C_{22}H_{37}B_3Mo_2O_2+H]^+$. Although mass spectrometric data along with all other the spectroscopic data provided some tips about nature of the molecule **2**, the core geometry was established when the single crystal X-ray diffraction analysis was carried out.

The X-ray analysis of **2** revealed a linear triborane $[B_3H_7]$, stabilized in the coordination sphere of two Mo atoms that depicted a trigonal bipyramidal $[Mo_2B_3]$ core geometry (Figure 1). One of the boron atoms (B2) and two metals (Mo1, Mo2) occupy the equatorial positions of the trigonal bipyramid, while other two boron atoms (B1 and B3) are placed at the axial positions. The avg. B-B bond distance in the triborane chain of **2** (1.736 Å) is shorter as compared to the avg. B-B bond distance of $[B_3H_7Fe_2(CO)_6]$ (1.778 Å)[13] and $[1,2\text{-}(Cp^*Ru)_2B_3H_7(\mu\text{-}H)_2]$ (1.920 Å)[14]. The Mo-Mo bond distance of 3.0326(6) Å is analogous to that of $[\{Cp(CO)_2Mo\}_2\{\mu\text{-}\eta^2\text{:}\eta^2\text{-}P_2\}]$ (3.036(2) Å)[15], however, it is shorter than that of $[CpMo(CO)_3]_2$ (3.235 Å)[16], $[Mo_2(CO)_{10}]^{2-}$ (3.123(7) Å)[17] and $[(Cp^*MoCl)_2B_3H_7]$, **I** (3.095(12) Å)[18]. In addition to Cp* ligand, both the Mo centers are ligated to one CO ligand. Interestingly, unlike $[(Cp^*MCO)_2B_4H_4(\mu\text{-}H)_2]$ (M = Cr, Mo), the CO ligands are positioned trans to each other in **2**, which is reflected in torsional angle of 172.79°(C-Mo-Mo-C). As a result, Cp* coordinated to Mo2, inclined towards the open face of B_3H_7 to minimize steric hindrance. This resulted two different Cp* environments, which was also evidential from ^1H and ^{13}C NMR spectra. This trans orientation of both CO and Cp* ring is quite unique; which was not observed in analogous $[(Cp^*MoCl)_2B_3H_7]$, **I**[18].

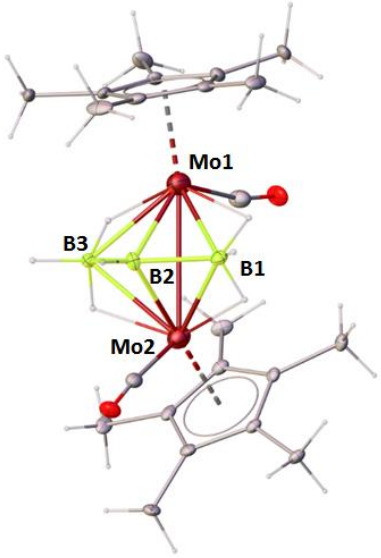

Figure 1. Molecular structure and labeling diagram of **2**. Selected bond lengths (Å) and angles (°): Mo1-Mo2 3.0326(6), Mo1-B1 2.354(5), Mo1-B2 2.207(5), Mo1-B3 2.351(6), B1-Mo2 2.319(5), B2-Mo2 2.253(5), B3-Mo2 2.338(5), B1-B2 1.715(8), B2-B3 1.757(7); Mo1-B1-Mo2 80.93(16), Mo1-B2-Mo2 85.67(17), B1-B2-B3 127.5(4).

In an effort to isolate the key molybdaborane intermediates during the formation of $[(Cp^*Mo)_2B_5H_9]$[19], Fehlner and co-workers isolated electronically unsaturated

Table 1. Important geometrical and spectroscopical parameters of some transition metal triborane complexes.

M_2B_3 clusters	Geometry, SEP	Structural Parameter	Spectroscopic data	Ref.

		$d_{av.M-M}$ (Å)	$d_{av.B-B}$ (Å)	^{11}B NMR (ppm)	^{1}H NMR[a] (ppm)	
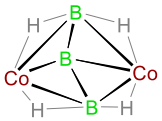	*nido*, 7	-	1.703	-18.1, 65.8	-12.70	21
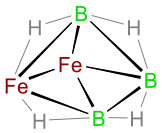	*nido*, 7	2.559	1.778	4.2, 12.1	-2.60, -16.60	13
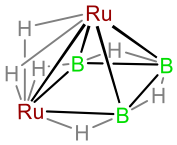	*nido*, 7	2.814	1.920	-2.5, -0.5	-4.06, -11.30, 13.60	14
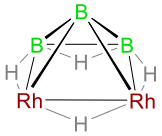	*nido*, 7	2.849	1.751	14.9, 43.9	-2.04, -12.09	14
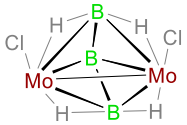	*closo*, 5	3.095	1.839	34.2, 105.5	-4.80	18
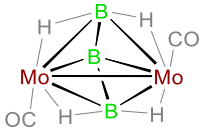	*closo*, 6	3.032	1.736	-3.7, 12.9	-13.08	This work

Co = Cp*Co, Fe = $Fe(CO)_3$, Rh = Cp*Rh, Ru = Cp*Ru, Mo = Cp*Mo, *a* = ^{1}H NMR chemical shifts for M-*H*-B (M=gr 6-9 transition metal), $d_{av.}$ = Average distance.

$[(Cp^*MoCl)_2B_3H_7]$ and $[(Cp^*MoCl)_2B_4H_{10}]$.[18] Subsequently, we suggested that the intermediate is rather a saturated $[(Cp^{\#}Mo)_2B_4H_{10}]$[20] instead of unsaturated $[(Cp^{\#}Mo)_2B_4H_8]$ ($Cp^{\#}$ = Cp or Cp*). Thus, the search for saturated form of another intermediate as such $[(Cp^*MoCl)_2B_3H_7]$, **I** became fascinating. Interestingly, $[\{Cp^*Mo(CO)\}_2\{\mu\text{-}\eta^3\text{:}\eta^3\text{-}B_3H_7\}]$, **2** was found to be isostructural with **I**. Hence, an insight into the cluster valence electrons (CVE) and skeletal electron pair (SEP) count of **2** became of interest. According to Wade skeleton electron counting rule, the SEP count required for the trigonal bipyramid $[M_2B_3]$ core is six (CVE = 42). Thus, cluster **2** is electronically saturated with 42 CVE and 6 SEP.

Occurrence of saturated $[Mo_2B_3]$ cluster **2** allowed us to compare it with other $[M_2B_3]$ clusters based on geometry, structural parameter, electron count and spectroscopic data (Table 1).[13,14,18,21] Apart from **2** and **I**, all other $[M_2B_3]$ clusters are manifested as *nido*-square pyramid geometry consisting 7 SEP. However, metals are located at different vertices in all these *nido*-$[M_2B_3]$ clusters. For instance, $[2,3\text{-}(Cp^*Rh)_2B_3H_7]$[14] exhibited as 7 SEP *nido*-square pyramid geometry comprised of M-M bond but $[2,3\text{-}(Cp^*Co)_2B_3H_7]$[21] reflected the same geometry without any M-M bond. This may be because of more feasibility in overlap between metal d-orbitals when coming down the group in periodic table. To sum up, we can propose that compound **2** is the first reported *closo*, saturated and unsubstituted dimetallic triborane species. Although **2** and **I** show structural resemblances, they display different $^{11}B\{^1H\}$ chemical shifts. The $^{11}B\{^1H\}$ chemical shifts of **2**, appeared at δ = 12.9 and -3.7 ppm in ~2:1 ratio, are significantly upfield shifted as compared to the corresponding $^{11}B\{^1H\}$ chemical shifts for **I** that appeared at δ = 105.5 and 34.2 ppm.[18] Cluster **2** rather exhibits similar kind of upfield ^{11}B resonances like other $[M_2B_3]$ clusters listed in Table 1.[13,14,18,21] Therefore, in order to assign the ^{11}B chemical shifts of **2** and **I**, we have carried out the ^{11}B NMR calculations using gauge invariant atomic orbital (GIAO) method that corroborate well with the experimental ^{11}B chemical shift values (Table S2).

In order to investigate the electronic and steric effect, we have carried out DFT calculation of **I** and **2** using b3lyp/def2-tzvp level of theory. All the structural parameters are quite comparable with that of solid-state X-ray structures. The MO analysis suggests that the additional pair of electrons of **2** is accommodated in one of the unoccupied orbitals of unsaturated cluster **I** and gets stabilized. In addition to that, the HOMO-LUMO gap is also remarkably

lower for **I** (2.439 eV) than **2** (3.370 eV). Moreover, the HOMO-8 of **2** sketched a substantial bonding overlap between the boron p and metal d orbitals extended throughout the cluster (Figure 2(a)). This type of extended orbital interaction was absent in **I**. These phenomena may demonstrate the fact that saturation in such clusters provides a greater stability. Further, the NBO charge analysis shows that the oxidation state of molybdenum decreased as the ancillary ligand Cl has been replaced by CO. This eventually increases the natural charge of the boron atoms of **2** (Table S1). Thus, the above results support the upfield $^{11}B\{^1H\}$ chemical shift of **2**. On the other hand, the Laplacian plot of electron density along the B1–B2–B3 plane displayed bond critical points (BCPs) and bond path connecting all these boron centers that represent the strong bonding along the triborane unit {Figure 2(b)}, which was further supported by WBI values of particular bonds. Again, a region of charge concentration has been detected along the B1–B2 and B2–B3 bonds. It shows high covalent character which is also reflected by the average electron density [ρ_r] value of 0.132 and a negative the energy density [H(r)] of -0.092.

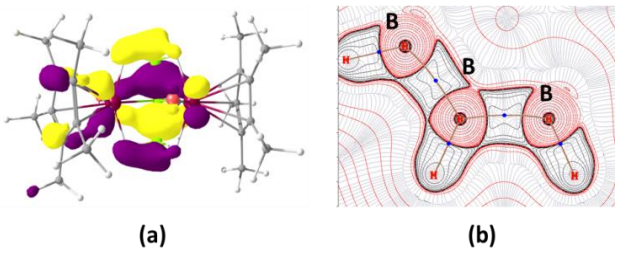

Figure 2. (a) HOMO-8 of **2** and (b) contour line diagram along the B1–B2–B3 plane obtained from Laplacian of electron density of **2**. [Charge concentration ($\nabla^2\rho(r) < 0$) regions have been represented by solid red lines, while the areas of charge depletion ($\nabla^2\rho(r) > 0$) are shown as dashed black lines. Blue dots and bold dark-brown lines depict BCPs and the bond path respectively].

Subsequently, in search for a probable existence of the tungsten analogue of saturated **2**, we have optimized [{Cp*W(CO)}$_2${μ-η^3:η^3-B_3H_7}] **II**. The B-B bond distance is marginally lower in **II** compared to **2** and it shows a significant decrease in $\Delta E_{HOMO\text{-}LUMO}$ by 0.517 eV from Mo analogue **2,** which occurred mainly due to the notable destabilization of HOMO. The HOMOs of both **2** and **II** are localized on the B–B bonds and the d-orbitals of the metal centers. As WBI (Table S1) values suggested the B-B bonding interaction to be more prominent in **II**, the destabilization of HOMO may be defined by the presence of higher energy 5d orbitals localized on tungsten atom (**II**) in place of 4d orbital of Mo atom (**2**). These phenomena indirectly suggest a reduced kinetic stability for **II** than **2**, which may be the reason for non-existence of the triborane analogue of tungsten.

Reactivity of [Cp*MoCl$_4$] with Co$_2$(CO)$_8$. As part of our effort to synthesize metal-rich metallaborane starting from transition metal stabilized tris-boranes, we tried the reactivity of **2** with different metal carbonyl fragments. These reactions led to the formation of various air-sensitive compounds with poor yield, which we were unable to isolate in pure form. As a result, in search for a different and efficient synthetic strategy from smaller metallaboranes to metal rich metallaborane we investigated the reactivity of metal carbonyls with in-situ generated intermediate, produced from the reaction of [Cp*MoCl$_4$] and [LiBH$_4$·THF]. Thermolysis of the intermediate with Co$_2$(CO)$_8$ led to the formation of hydrido(hydroborylene) **5**, μ_4-boride **6**, triple-decker sandwich complex **7** and bimolybdenametallaborane **8** (Scheme 2). Preparative thin-layer chromatography was used to separate all products for further spectroscopic and structural characterization. Detailed spectroscopic and structural characterization of these species are described below.

Triply-bridging hydrido(hydroborylene), 5. Compound **5** was isolated as green solid in moderate yield. The ^{11}B NMR spectrum reveals a broad downfield resonance peak at δ = 69.7 ppm. In addition to that, the presence of a peak at δ = 1.86 ppm in ^1H NMR confirmed one Cp* environment. Further, there is a peak at *m/z* 731.9764 in mass spectrum that corresponds to [$C_{29}H_{31}O_9Mo_2CoB$]$^+$. These data indicate that the structural framework contains two Cp*Mo unit. Apart from one up field chemical shift at δ = -11.31 ppm, the ^1H NMR also revealed a downfield broad peak at δ = 10.41 ppm. This could result from the existence of B-H_t.[21,22] The broadened nature of the ^{11}B peak and the ^1H chemical for shifts due to terminal B-*H* protons support the existence of borylene moiety in **5**. All these spectral information was abstruse to get a proper view on complete structure. Thus, the X-ray diffraction study explicitly guided us to understand the structural framework.

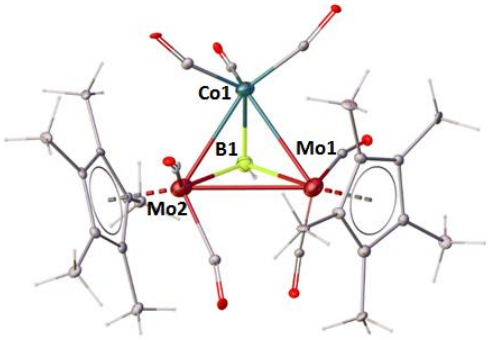

Figure 3. Molecular structure and labeling diagram of **5**. The bridging H-atom is not located. Selected bond lengths (Å) and angles (°): B1-Co1 2.04(2), B1-Mo2 2.23(3), B1-Mo1 2.25(3), Mo1-Mo2 3.058(8). Co1-B1-Mo2 80.5(8), Co1-B1-Mo1 81.2(10), Mo2-B1-Mo1 86.2(9), B1-Co1-Mo2 52.7(10).

Scheme 2. Synthetic route to metal rich metallaborane. (Carbonyls and Mo-Mo bonds are not shown for clarity in 7 and 8).

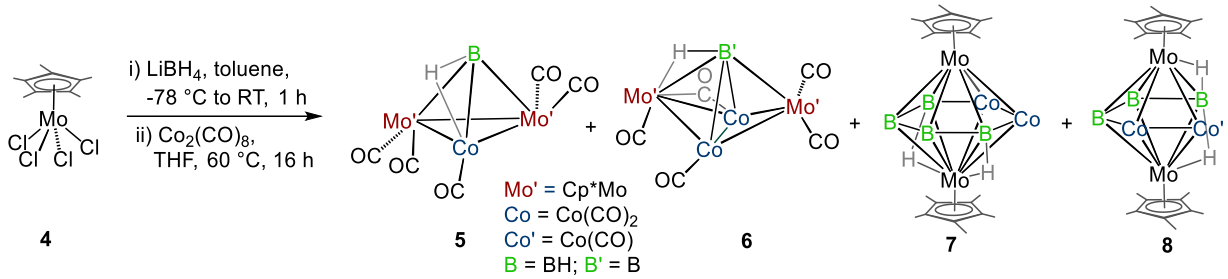

As shown in Figure 3, **5** can be represented by formulae [{Cp*Mo(CO)$_2$}$_2$Co(CO)$_3$BH(μ-H)], owning tetrahedral core geometry, where boron atom occupied the peak of the pyramid connected to trimetallic trigonal plane (Mo-Co-Mo). Although the Co-*H*-B has not been located in X-ray, ^{1}H-NMR peak at δ = -11.31 ppm clearly signified the occurrence of Co-H-B. So based on the structural parameters as well as spectroscopic data, we describe compound **5** as triply bridging hydrido(hydroborylene) species. The Co-B bond distance is slightly closer to boron-rich cobaltaboranes[8d] and hydrido(hydroborylene)[23] species reported by us. Earlier, Braunschweig[24] and Tobita[25] group have synthesized a series of mono and binuclear hydrido(borylene). Recently, we have also developed a typical synthetic strategy for the synthesis of triply bridging borylene and hydrido(borylenes) species.[26] Note that the ^{11}B chemical shift for **5** that appeared at δ = 69.7 ppm is in the upfield region as compared to reported [(Cp*Rh)$_2${Co$_2$(CO)$_4$}(μ-CO)(μ_3-CO)(μ_3-BH)][23] and [{Cp*W(CO)$_2$}$_2${Fe(CO)$_2$}(μ_3-BH)$_2$H$_2$].[26a]

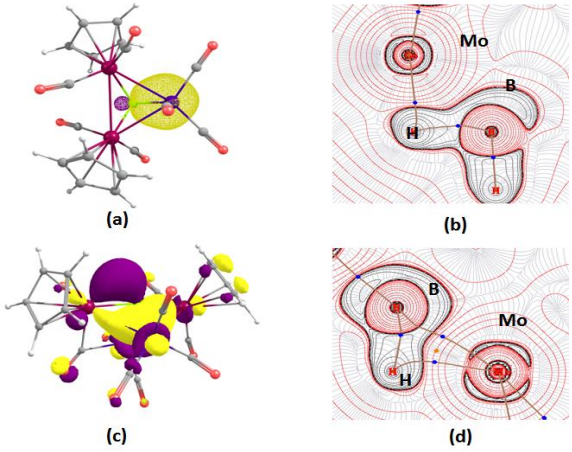

Figure 4. (a) 3c-2e bonding interaction of Co-H-B in **5**; (c) HOMO-18 of **6**, showing extended bonding overlap over molecular framework; (b) and (d) represent contour line diagram along the M–H–B planes of **5** and **6** respectively, obtained from Laplacian of electron density.

To get some insight into the borylene character as well as bonding scenario, we have performed the DFT calculation on b3lyp/def2-tzvp level of theory. Although, the MO analysis shows a head to head overlap between the d orbital of Co and the p orbital of B, the Co-B separation of (2.133 Å) in the optimized structure of **5** is significantly longer in comparison to its solid-state structure (2.04(2) Å). This σ bonding interaction was further supported by WBI value of 0.413. In addition, there is one 3c-2e bonding interaction along Co-*H*-B (Figure 4(a)). The NBO studies also supported a greater contribution of B (31.83%) than Co (26.63%) in the Co-*H*-B banana bond. Further, from the topological analysis, we have noticed a shift of BCP towards H atom along the Co-H bond path. This clearly signifies that the bond is more polarized towards hydridic hydrogen than Co-center. Based on all these theoretical outputs, it is apparent that the B-H interaction is more prominent than Co-H within the Co-*H*-B 3c-2e bonding scenario.

Tetrametallic μ_4-Boride, 6. Beside the triply bridging hydrido(hydroborylene) species, another moderately air stable black solid was also yielded in 11% yield. The mass spectrum shows an intense ion peak at *m/z* 844.8936 that corresponds to [C$_{27}$H$_{32}$BO$_7$Mo$_2$Co$_2$]$^+$. The ^{1}H NMR spectrum displays single peak at δ=1.93 ppm in Cp* region along with one upfield region shift at δ=-3.27 ppm. The presence of CO and Cp* ligand was further confirmed from ^{13}C NMR and IR spectroscopic data. Further, a downfield single resonance shift was recorded at δ = 129.5 ppm in room temperature ^{11}B NMR, which demonstrates the presence of metal rich environment around boron. The observed ^{11}B chemical shift is in agreement with some of the structurally characterized boride clusters.[26,28]

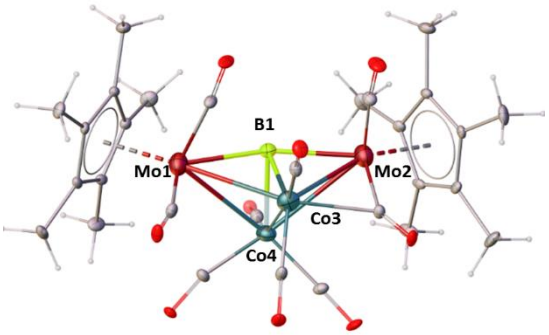

Figure 5. Molecular structure and labeling diagram of **6**. The bridging H-atom is not located. Selected bond lengths (Å) and angles (°):Mo1-B1 2.180(5), Mo1-Co3 2.8839(8), Mo1-Co4 2.7023(8), Mo2-Co3 2.967(5), Mo2-B1 2.125(5), Co3-B1 2.022(5), Co4-B1 2.076(5). B1-Mo1-Co4 48.92(14), Co4-Mo1-Co3 52.00(2), Mo2-B1-Mo1 163.7(3), Co4-B1-Co3 73.57(17).

Along with the spectroscopic details, the X-ray structure analysis also led us to the confirmation about the solid-state structure. As shown in Figure 5, the crystal structure of **6** can be described as heterometallic boride cluster having a boron atom placed at semi-interstitial position of butterfly M$_2$M'$_2$ core (M= Mo, M' = Co). The observed Mo-B (2.41Å) and Co-B (2.05Å) bond distances are consistent with the known molybdaboranes, cobaltaboranes and other reported μ_4-boride clusters.[27,18b,29] The boron atom is situated at semi-interstitial position in quite bent fashion because of

Mo1-B1-Mo2 angle of 163.7°. Cluster **6** comprises of 62-CVE. And it is isostructural as well as isoelectronic to recently reported [{Cp*W(CO)$_2$}$_2${Co$_2$(CO)$_5$}(μ_4-B)(μ_2-H)].[29a]

To investigate the stability of this boride cluster, we have carried out molecular orbital analysis. As shown in Figure 4(c), the HOMO-18 showed an extended overlap between the d orbitals of metal centers and p orbital of semi-interstitial boron atom. In addition, the presence of 3c-2e bonding scenario has also been observed along the Mo-H-B. Interestingly, unlike **5**, there was no shift of BCP observed along the Mo-H bond.

In addition to the formation of these species, the reaction also yielded a triple-decker species **7**[29b], which was reported recently based on spectroscopic data. Thus, in an attempt to get the X-ray structure, we have carried out the XRD analysis of **7**. The solid-state X-ray structure of **7** represented as [(Cp*Mo)$_2${μ-η^6:η^6-Co$_2$(CO)$_5$B$_4$H$_4$}(μ-H)$_2$] possessing two {Cp*Mo} fragments sandwiched hexagonal planar [Co$_2$(CO)$_5$B$_4$H$_4$] middle deck (sum of internal angles = 720°) {Figure 6(left)}. The μ_2-bridged carbonyl connected to two cobalt center is inclined towards Mo2 atom. The eclipsed alignment of terminal CO in Co$_2$(CO)$_5$ has also been found in **7**. In comparison to some reported dimolybdenaboranes, the Mo-Mo bond distance of 2.790 Å is smaller as compared to, which is also supported by higher WBI values (Table S1).

Metal-rich dimolybdaborane cluster, 8. Along with metal-rich metallaborane clusters **5**, **6** and triple decker sandwich complex, **7**, the reaction also yielded compound **8** as a brown solid in 12% yield. In the ESI-MS of **8**, a molecular ion peak has been recorded at *m/z* = 786.9598. The ^{11}B{^{1}H} NMR spectrum of **8** showed three signals at δ = 102.5, 100.0 and 30.3 ppm in ~1:1:1 ratio signifying the existence of three distinct boron environments. The ^{1}H NMR spectrum revealed one kind of Cp* ligand at δ = 2.00 ppm in addition to the resonance peak for B-H$_t$ protons at δ = 6.89 ppm. The presence of an up-field chemical shift at δ = -13.44 ppm in the ^{1}H NMR may be due to the presence of Mo-*H*-B protons. The ^{13}C NMR and IR spectrum further confirmed the existence of both bridging and terminal CO ligands. However, a definite inference eluded us until the cluster core has been revealed by single-crystal X-ray analysis.

As shown in Figure 6 (middle), the molecular structure of **8** can be defined as [(Cp*Mo)$_2$Co$_2$(CO)$_3$(μ-CO)$_3$B$_3$H$_3$(μ-H)$_2$]. It is consistent with the spectroscopic output and structurally and electronically analogous to ditungstenaborane,[29b] recently reported by us. The structure can be portrayed as a *nido* hexagonal bipyramid with atoms Co1, Co2, B1, B2 and B3 constituting the open and flattened base. Mo1 and Mo2 capped above and below of the base respectively. Applying classical skeletal electron counting formalism[12], using 8-vertex *oblato-closo* hexagonal bipyramid as starting point, cluster **8** can be represented as electron deficient 6-SEP *oblato-nido*-species. Although the avg. Mo-B-Mo bond angle in **8** is shorter as compared to [{Cp*Mo(CO)}$_2${μ-η^3:η^3-B$_3$H$_7$}], **1**, it is larger compared to [(Cp*Mo)$_2${μ-η^6:η^6-Co$_2$(CO)$_5$B$_4$H$_4$}(μ-H)$_2$], **7.** Further, the Mo-Mo separation of (2.8489(9) Å) is shorter as compared

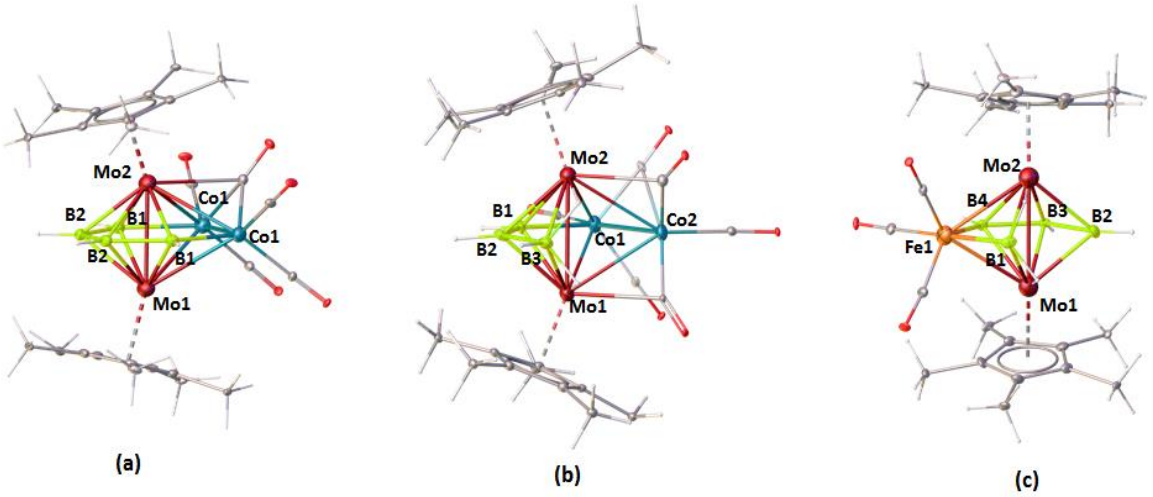

Figure 6. Molecular structure and labeling diagram of **7** (left), **8** (middle) and **9** (right). Selected bond lengths (Å) and angles (°) of **7**: Mo1-Mo2 2.7900(4), Mo1-B1 2.329(3), Mo1-B2 2.181(3), B1-Mo2 2.273(3), B2-Mo2 2.205(3), Co1-Co2 2.5110(6), Co1-Mo1 2.7958(4), B1-Co1 2.112(3), B1-B2 1.715(8); Mo1-B1-Mo2 74.63(9), Mo1-B2-Mo2 79.01(9). Selected bond lengths (Å) and angles (°) of **8**: Mo1-Mo2 2.8489(9), Mo1-B1 2.247(8), Mo1-B2 2.186(8), Mo1-B3 2.285(8), Co1-Co2 2.4341(13), Co1-Mo1 2.7032(12), B1-Co1 2.022(8); Mo1-B1-Mo2 78.8(3), Mo1-B2-Mo2 81.4(3), Mo1-B3-Mo2 76.8(3). Selected bond lengths (Å) and angles (°) of **9**: Mo1-Mo2 2.7965(18), Mo1-B1 2.41(2), Mo1-B2 2.25(2), Mo1-B3 2.170(18), Mo1-B4 2.22(2), Mo1-Fe1 2.668(3), Fe1-B1 2.12(2), Fe1-B4 2.05(2); Mo2-B1-Mo1 70.9(5), Mo2-B4-Mo1 78.4(6).

to [(Cp*Mo)$_2$(CO)(μ-Cl)W(CO)$_4$B$_3$H$_4$],[20] however, it is longer as found in [(Cp*Mo)$_2$Se$_2$(SeCH$_2$Ph)B$_4$H$_3$] and [(Cp*Mo)$_2$Te$_2$B$_4$H$_4$][30].

In a similar fashion, the reaction of Fe$_2$(CO)$_9$ with the *in-situ* generated intermediate, produced from [Cp*MoCl$_4$] with LiBH$_4$ reaction, at 60 ˚C led to the formation of an air and moisture sensitive product **9**.[31] Note that, compound **9** and known [(Cp*Mo)$_2$B$_5$H$_9$] couldn't be separated by chromatographic methods. Hence, they were isolated as inseparable solids and crystallized from a CH$_2$Cl$_2$/hexane solution at –5 °C. Two different types of crystals were obtained; crystals of **9** is black and [(Cp*Mo)$_2$B$_5$H$_9$] is orange. The X-ray

diffraction analysis suggested that the structural formulae for **9** can be defined as $[(Cp^*Mo)_2B_4H_8Fe(CO)_3]$. As shown in Figure 6(right), **9** can be represented as bicapped trigonal bipyramidal geometry. Two Mo atoms and B4 are placed at equatorial position of the trigonal bipyramid and the axial B1 and B2 atoms capped the {Mo1Fe1Mo2} and {Mo1B3Mo2} triangular faces, respectively. Interestingly, **9** is isostructural with $[(Cp^*W)_2B_4H_8Fe(CO)_3]$[32] in which two Mo atoms occupied the same position as that of W. Cluster **9** follows the electron counting rule with total cluster valance electron of 56 (6 SEP). The Mo-Mo bond distance of 2.7969(18) Å is also comparable to other reported dimolybdenaborane containing 6 SEP.

Further, all the spectroscopy data of **9** corroborated well with X-ray structure. For example, four intense boron resonances of **9** appeared at δ = 93.0, 83.1, 38.9, and 34.5 ppm signify the presence of four boron atoms having different environments. The ^{1}H NMR spectrum showed a peak at δ = 2.07 ppm due to the presence of single Cp* environment. In addition, two upfield region peaks at δ = -5.96 and -12.36 ppm in the ^{1}H NMR correspond to bridging Mo-*H*-B hydrogens. Further, the IR spectrum of **9** revealed the presence of terminal CO ligand at ν = 1988, and 1918 cm^{-1}. The mass spectrum showed molecular ion peak at *m/z* = 655.0757 which correspond to $[M+H]^+$.

CONCLUSION

In this article, we have explained the isolation and structural characterization of a linear triborane species stabilized in the coordination sphere of two molybdenum atoms. Structural insight obtained from X-ray diffraction analysis, revealed that a B_3H_7 unit is ligated in η^3–fashion to both of the metal centre. Cluster $[\{Cp^*Mo(CO)\}_2\{\mu\text{-}\eta^3\text{:}\eta^3\text{-}B_3H_7\}]$, **2** is an unique addition to the series of linear triborane species which show distinct electronic as well as structural features. Despite of having structural resemblances with $[(Cp^*MoCl)_2B_3H_7]$, **2** is considered novel due to its electronic saturation. Additionally, theoretical studies demonstrated the plausible explanation for the stability. Further, we have demonstrated a different and efficient approach to synthesize metal-rich heterometallic metallaborane clusters that led to the formation of triply bridging trimetallic hydrido(hydroborylene), **5** and tetrametallic μ_4-boride, **6**. NMR studies and a detailed theoretical investigation explicitly explained a lower borylene character of **5** compared as compared to other reported hydrido(borylenes) species.

EXPERIMENTAL SECTION

General Procedures and Instrumentation. All reactions and experiments were performed under an inert atmosphere or in vacuo using standard Schlenk line techniques and glove box. THF, toluene and hexane were among the solvents those were first dried utilising appropriate drying agents (sodium/benzophenone) and then distilled under argon environment. Three cycles of freeze-pump-thaw degassed $CDCl_3$, which was then reserved over molecular sieves. $[Cp^*Mo(CO)_3Me]$[33] and $[Cp^*MoCl_4]$[34] were synthesized following the literature methods. Meanwhile, other chemicals like $[LiBH_4{\cdot}THF]$, $[Co_2(CO)_8]$ and $[Fe_2(CO)_9]$ were obtained from commercial source (Aldrich) and used exactly as it was given without further purification. Preparative thin layer chromatography was performed for the separation of products (20 x 20 cm). It was made of Merck 105554 TLC silica gel 60 F_{254} layer, having thickness of 250 μm on aluminium sheets. NMR spectra were recorded on 400 and 500 MHz Bruker FT-NMR spectrometers. The residual solvent protons functioned as reference (δ, ppm, d_6-benzene, 7.16; $CDCl_3$, 7.26). ^{1}H decoupled ^{11}B spectra were processed with a backward linear prediction algorithm to remove the broad ^{11}B background signal of the NMR tube. The infrared spectra were recorded on a Nicolet iS10 spectrometer. Agilent 6545 Q-TOF LC/MS instrument recorded Electrospray mass (ESI-MS) spectra.

Synthesis of 2. In a flame-dried Schlenk tube, $[Cp^*Mo(CO)_3Me]$, (0.1 g, 0.30 mmol) dissolved in 15 mL of toluene was reacted with 1.2 equiv. (2.4 mL) of $[LiBH_4{\cdot}THF]$ at -78 °C and allowed to stir for 1 h at room temperature and then by addition of $[BH_3{\cdot}THF]$ (1 mL, 10 mmol) it was left to stir for additional 24 h. The volatile components were evaporated using vacuo and then hexane/dcm was added into the residue to dissolve as much as possible. It was then extracted through Celite using a frit. The extracted filtrate was then dried and put through a chromatographic work-up utilising TLC plates made of silica gel. Elution with full hexane mixture afforded the compound in order of elution: green **2** (0.010 g, 12%) along with *arachno*-$[Cp^*Mo(CO)_2B_3H_8]$[10c] (0.022 g, 23%) and $[(Cp^*Mo)_2B_5H_9]$[19] (0.016 g, 21%).

2: MS (ESI$^+$): *m/z* calculated for $[M+H]^+$ 558.1217, found 558.1215; ^{11}B{^{1}H} NMR (160 MHz, $CDCl_3$, 22 °C): δ = 12.9 (s, 2B), -3.7 ppm (s, 1B); ^{1}H NMR (500 MHz, $CDCl_3$, 22 °C): δ = 3.01 (br, 2H, BH_t), 1.57 (br, 1H, BH_t) 2.02 (s, 15H, C_5Me_5), 1.90 (s, 15H, C_5Me_5), -13.08 ppm (br, 4H, Mo-*H*-B); ^{13}C{^{1}H} NMR (22 °C, 125 MHz, $CDCl_3$): δ = 236.5 (s, *C*O), 233.7 (s, *C*O), 103.7 (s, C_5Me_5), 103.3 (s, C_5Me_5), 11.8 (s, C_5Me_5), 11.7 ppm (s, C_5Me_5); IR (CH_2Cl_2, cm^{-1}): 2475 (w, BH_t), 1638 (CO).

Synthesis of 5-8: At first, $[Cp^*MoCl_4]$, (0.1 g, 0.27 mmol) was weighed in a flame-dried Schlenk tube and dissolved in 10 mL of toulene. Five-fold excess of $[LiBH_4{\cdot}THF]$ (0.7 mL) was slowly added dropwise into it at -78 °C and the mixture was then stirred at room temperature for 1 h. The volatile components were evaporated using vacuo and then hexane was added into the residue to dissolve as much as possible. It was then extracted through Celite using a frit. After drying hexane, we got the brownish-green coloured extract. Later, 10 mL of THF solution of $[Co_2(CO)_8]$ (0.03 g) was transferred to extracted mixture using argon flow. The thermolysis of whole mixture was carried out for 16 h at 60 °C. The solvent was eliminated using vacuum, and the residue was then extracted into hexane/dcm which was passed through Celite. The extracted filtrate was then dried and put through a chromatographic work-up utilising TLC plates made of silica gel. Elution with a hexane/CH_2Cl_2 (70:30 v/v) mixture yielded, well separated greenish brown **5** (0.007 g, 7%), black **6** (0.012 g, 11%), brown **7** (0.014 g, 15%), brown **8** (0.013 g, 12%) along with $[(Cp^*Mo)_2B_5H_9]$[19] (0.017 g, 24%).

5: MS (ESI+): *m/z* calculated for $[M+H]^+$ 731.9777, found 731.9764; ^{11}B{^{1}H} NMR (160 MHz, $CDCl_3$, 22 °C): δ = 69.7 (*s*, 1B); ^{1}H NMR (500 MHz, $CDCl_3$, 22 °C): δ = 10.41 (br, 1H, B-H_t), 1.86 (s, 30H, C_5Me_5), -11.31 (br, 1H, Mo-*H*-B); ^{13}C{^{1}H} NMR (22 °C, 125 MHz, $CDCl_3$): δ = 101.8 (C_5Me_5), 9.6 ppm (C_5Me_5); IR (CH_2Cl_2, cm^{-1}): 2446 (w, BH_t), 2020, 1959 (CO).

6: MS (ESI+): *m/z* calculated for $[M+H]^+$ 844.8938, found 844.8936; ^{11}B{^{1}H} NMR (160 MHz, $CDCl_3$, 22 °C): δ = 129.5 (*s*, 1B); ^{1}H NMR (500 MHz, $CDCl_3$, 22 °C): δ = 1.93 (s, 30H, C_5Me_5), -3.27 (br, 1H, Mo-*H*-B); ^{13}C{^{1}H} NMR (22 °C, 125 MHz, $CDCl_3$): δ = 103.9 (C_5Me_5), 10.8 ppm (C_5Me_5); IR (CH_2Cl_2, cm^{-1}): 2023, 1988 (w, BH_t), 1793, 1752 (CO).

8: MS (ESI+): *m/z* calculated for $[M+H]^+$ 786.9601, found 786.9598; ^{11}B{^{1}H} NMR (160 MHz, $CDCl_3$, 22 °C): δ = 102.5 (s, 1B), 100.0 ppm (s, 1B), 30.3 (s, 1B); ^{1}H NMR (500 MHz, $CDCl_3$, 22 °C): δ = 6.89 (br, 3H, B-H_t), 2.00 (s, 30H, C_5Me_5), -13.44 ppm (br, 2H, Mo-*H*-B); ^{13}C{^{1}H} NMR (22 °C, 125 MHz, $CDCl_3$): δ = 110.1 (C_5Me_5), 12.2 (C_5Me_5); IR (CH_2Cl_2, cm^{-1}): 2490, 2450 (w, BH_t), 2012, 1992, 1829, 1639 (CO).

Synthesis of 9: At first, $[Cp^*MoCl_4]$, (0.1 g, 0.27 mmol) was weighed in a flame-dried Schlenk tube and dissolved in 10 mL of toulene. Five-fold excess of $[LiBH_4{\cdot}THF]$ (0.7 mL) was slowly added

dropwise into it at -78 °C and the mixture was then stirred at room temperature for 1 h. The volatile components were evaporated using vacuo and then hexane was added into the residue to dissolve as much as possible. It was then extracted through Celite using a frit. After drying hexane, we got the brownish-green coloured extract. Later, 10 mL of THF solution of $[Co_2(CO)_8]$ (0.03 g) was transfered to the extracted mixture using argon flow. The thermolysis of whole mixture was carried out for 16 h at 60 °C. The solvent was eliminated using vacuum, and the residue was then extracted into hexane/dcm which was passed through Celite. The extracted filtrate was then dried and put through a chromatographic work-up utilising TLC plates made of silica gel. Elution with a hexane/CH_2Cl_2 (70:30 v/v) mixture yielded black **9** (0.009 g, 11%) along with the known $[(Cp^*Mo)_2B_5H_9]$[19] (0.017 g, 24%).

9: MS (ESI+): *m/z* calculated for **9** 655.0757, found 655.0763; $^{11}B\{^1H\}$ NMR (160 MHz, $CDCl_3$, 22 °C): δ = 93.0 (s, 1B), 83.1 ppm (s, 1B), 38.9 (s, 1B), 34.5 ppm (s, 1B); ^1H NMR (500 MHz, $CDCl_3$, 22 °C): δ = 4.46 (br, 2H, B-H_t), 6.54 (q, 2H, B-H_t) 2.07 (s, 30H, C_5Me_5), -5.96 ppm (br, 2H, *Mo-H*-B), -12.36 ppm (br, 2H, *Mo-H*-B); $^{13}C\{^1H\}$ NMR (22 °C, 125 MHz, $CDCl_3$): δ = 107.2 (C_5Me_5), 12.0 (C_5Me_5) ; IR (CH_2Cl_2, cm^{-1}): 2458 (w, BH_t), 1988, 1918 (CO).

X-ray Analysis Details. Slow diffusion of a hexane-CH_2Cl_2 solution of **2**, **5**-**9** compound was applied to grow quality crystals which are suitable for XRD analysis. The crystal data collection of **2**, **6** and **7** was done in Bruker AXS Kappa APEXII CCD diffractometer. For **5** and **8**, collection and integration of crystal data were performed using a D8 VENTURE Bruker AXS diffractometer with graphite monochromated Mo-Kα (λ = 0.71073 Å) radiation at 150(2) K. Bruker Kappa APEXIII was used to collect as well as integrate the crystal data of **9**. In order to solve the structures, dual-space algorithm using SHELXT program[35] was used and refinement was achieved utilizing full-matrix least-squares methods based on F2 (SHELXL program)[36]. The molecular structures were drawn using Olex2.[37] Whereas, anisotropic displacement parameters assisted for refinement of the non-hydrogen atoms, the hydrogen atoms except bridging hydrogen were introduced through Fourier difference maps analysis. H atoms were finally included in their calculated positions and treated as riding on their parent atom with constrained thermal parameters. Crystallographic data have been deposited with the Cambridge Crystallographic Data Center as supplementary publication no CCDC- 1019009 (**2**), CCDC- 2183897 (**5**), CCDC- 2183896 (**6**), CCDC- 2183898 (**7**), CCDC- 2183894 (**8**), and CCDC- 2183895 (**9**). These data can be obtained free of charge from The Cambridge Crystallographic Data Centre via www.ccdc.cam.ac.uk/data_request/cif.www.ccdc.cam.ac.uk/data_request/cif.

Crystal data for **2**: $C_{22}H_{37}B_3O_2Mo_2$, M_r = 557.83, Triclinic space group *P-1*, a = 8.9262(10) Å, b = 9.7089(12) Å, c = 15.7243(18) Å, α = 72.239(4)°, β = 79.130(5)°, γ = 76.193(5)°, V = 1250.4(3) Å^3, Z = 2, ρ_{calcd} = 1.482 g/cm^3, μ = 1.017 mm^{-1}, F(000) = 568, R_1 = 0.0554, wR_2 = 0.1750, 9322 independent reflections [2θ≤49.20°] and 297 parameters.

Crystal data for **5**: $C_{27}H_{31}BO_7Mo_2Co$, M_r = 729.14, Orthorhombic space group *Pbca*, a = 10.800(2) Å, b = 17.380(4) Å, c = 30.260(6) Å, α = 90°, β = 90°, γ = 90°, V = 5680(2) Å^3, Z = 8, ρ_{calcd} = 1.705 g/cm^3, μ = 1.489 mm^{-1}, F(000) = 2920, R_1= 0.0960, wR_2 = 0.2556, 4572 independent reflections [2θ≤49.99°] and 394 parameters.

Crystal data for **6**: $C_{29}H_{30}BO_9Mo_2Co_2$, M_r = 843.08, Monoclinic space group *P21/n*, a = 9.0234(3) Å, b = 16.8366(4)Å, c = 21.9213(7) Å, α = 90°, β = 101.8121(14)°, γ = 90°, V = 3259.83(17) Å^3, Z = 4, ρ_{calcd} = 1.718 g/cm^3, μ = 1.800 mm^{-1}, F(000) = 1676, R_1 = 0.0410, wR_2 = 0.0907, 5739 independent reflections [2θ≤49.99°] and 398 parameters.

Crystal data for **7**: $C_{25}H_{34}B_4O_5Mo_2Co_2$, *Mr* = 767.50, Orthorhombic, space group *Pnma*, a = 16.8001(3) Å, b = 15.2353(3) Å, c = 11.5143(2) Å, α = 90°, β = 90°, γ = 90°, V = 2947.14(9) Å^3, Z = 4, ρ_{calcd} = 1.730 g/cm^3, μ = 1.970 mm^{-1}, F(000) = 1528, R_1 = 0.0196, wR_2 = 0.0533, 2696 independent reflections [2θ≤50.00°] and 198 parameters.

Crystal data for **8**: $C_{26}H_{35}B_3O_6Mo_2Co_2$, M_r = 785.77, Triclinic, space group *P-1*, a = 11.7113(17) Å, b = 16.662(2) Å, c = 16.920(3) Å, α = 114.781(6)°, β = 90.041(7)°, γ = 99.541(7)°, V = 2947.1(8) Å^3, Z = 4, ρ_{calcd} = 1.771 g/cm^3, μ = 1.976 mm^{-1}, F(000) = 1568, R_1 = 0.0531, wR_2 = 0.1315, 11161 independent reflections [2θ≤51.36°] and 755 parameters.

Crystal data for **9**: $C_{23}H_{30}O_3B_4Mo_2Fe$, M_r = 645.44, Monoclinic, space group *P2$_1$*, a = 10.5118(13) Å, b = 16.3058(18) Å, c = 16.700(2) Å, α = 90°, β = 102.664(5)°, γ = 90°, V = 2792.8(6) Å^3, Z = 4, ρ_{calcd} = 1.535 g/cm^3, μ = 1.418 mm^{-1}, F(000) = 1288, R_1 = 0.0540, wR_2 = 0.1487, 9788 independent reflections [2θ≤50.00°] and 596 parameters.

ASSOCIATED CONTENT

Supporting Information

On the ACS publication page at DOI: xxx, the supporting information is freely accessible. It includes comprehensive synthesis instructions, ^1H, $^{11}B\{^1H\}$, $^{13}C\{^1H\}$ NMR and mass spectra, as well as X-ray analysis details. DFT outputs for **2**-**9** and other computational details are also provided. This material can be accessed through the internet without any charge at http://pubs.acs.org

AUTHOR INFORMATION

Corresponding Author

*E-mail: sghosh@iitm.ac.in. Tel: +91-44-22574230. Fax: +91 44-22574202

Notes

The authors declare no competing financial interest.

ACKNOWLEDGMENT

This work was supported by SERB, (grant no. CRG/2019/001280) and the Centre of Excellence on Molecular Materials and Functions under the Institution of Eminence scheme of IIT Madras. S.M. acknowledges IIT Madras and S.G. thank CSIR for fellowships. We acknowledge the discussions and X-ray structure studies provided by Dr. V. Ramkumar, Dr. P.K.S. Antharjanam and Dr. B. Varghese. IIT Madras' computational facility is gratefully acknowledged.

REFERENCES

(1) (a) Neeve, E. C.; Geier, S. J., Mkhalid, I. A. I.; Westcott, S. A.; Marder, T. B. Diboron(4) Compounds: From Structural Curiosity to Synthetic Workhorse. *Chem. Rev.* **2016**, *116*, 16, 9091–9161. (b) Himmel, H.-J. Electron-Deficient Triborane and Tetraborane Ring Compounds: Synthesis, Structure, and Bonding. *Angew. Chem. Int. Ed.* **2019**, *58*, 11600–11617. (c) Yu, W.-B.; Cui, P.-F.; Gao, W.-X; Jin, G.-X. B-H activation of carboranes induced by late transition metals. *Coord. Chem. Rev.* **2017**, *350*, 300-319. (d) Cui, P.-F.; Lin, Y.-J.; Li, Z.-H; Jin, G.-X. Dihydrogen Bond Interaction Induced Separation of Hexane Isomers by Self-Assembled Carborane Metallacycles. *J. Am. Chem. Soc*. **2020**, *142*, 8532–8538. (e) Cui, P.-F.; Liu, X.-R.; Guo, S.-T.; Lin, Y.-J.; Jin, G.-X. Steric-Effects-Directed B–H Bond Activation of para-Carboranes. *J. Am. Chem. Soc.* **2021,** *143*, 5099–5105.

(2) Osorio, E.; Olson, J. K.; Tiznado, W.; Boldyrev. A. I. Analysis of Why Boron Avoids sp^2 Hybridization and Classical Structures in the B_nH_{n+2} Series. *Chem. Eur. J.* **2012**, *18*, 9677–9681.

(3) Hayashi, Y.; Segawa, Y.; Yamashita, M.; Nozaki, K. Syntheses and properties of triborane(5)s possessing bulky diamino substituents on terminal boron atoms. *Chem. Commun*. **2011**, *47*, 5888–5890.

(4) (a) Dewhurst, R. D.; Horl, C.; Phukan, A. K.; Pinzner, F.; Ullrich. S.; Braunschweig, H. Direct Hydroboration of B=B Bonds: A Mild Strategy for the Proliferation of B-B Bonds. *Angew. Chem. Int. Ed.* **2014**, *53*, 3241–3244. (b) Schmidt, U.; Werner, L.; Arrowsmith, M.; Deissenberger, A.; Hermann, A.; Hofmann, A.; Ullrich, S.; Mattock, J. D.; Vargas, A.; Braunschweig, H. trans-Selective Insertional Dihydroboration of a cis-Diborene: Synthesis of Linear sp3 -sp2 -sp3 -Triboranes and Subsequent Cationization, *Angew. Chem. Int. Ed*. **2020**, *59*, 325-329.

(5) (a) Shaykh, B. A. M.; Rheingold, A. L.; Haggerty, B. S.; Housecroft, C. E. Reactivity of palladium(II) complexes with bidentate bis(phosphine) ligands toward the octahydrotriborate(1-) anion and dependence of the reaction upon halide arrangement: molecular structure of the trans(bis (diphenylphosphino)hexane)palladium(II) dichloride dimer. *Inorg. Chem.* **1991**, *30*, 1, 125–130. (b) Haggerty, B. S.; Housecroft, C. E.; Rheingold, A. L.; Shaykh, B. A. M. Competition between Triborane as a Ligand and a Hydride Donor at Platinum Centres containing Chelating Phosphines: Molecular Structures of $[\{Ph_2P(CH_2)_2PPh_2\}PtB_3H_7]$, $[\{Ph_2P(CH_2)_4PPh_2\}PtB_3H_7]$ and $[Pt_2H_3\{(Ph_2PC_5H_4)_2Fe\}_2]Cl$. *J. Chem. Soc. Dalton Trans.* **1991**, 2175-2184.

(6) Gaines, D. F.; Hildebrandt, S. J. Low-Temperature Crystal and Molecular Structure of Tetracarbonyl [2-bromoheptahydrotriborato (1-)] manganese, $(CO)_4MnB_3H_7Br$, and a ^1H NMR Study of the Kinetics of Its Intramolecular Hydrogen Exchange in Solution. *Inorg. Chem.* **1978**, *17*, 794-806.

(7) Kar, S.; Bairagi, S.; Kar, K.; Roisnel, T.; Dorcet, V.; Ghosh, S. Metal Coordinated Tri- and Tetraborane Analogues. *Eur. J. Inorg. Chem.* **2021**, 4443–4451.

(8) (a) Trageser, T.; Bolte, M.; Lerner, H. –W.; Wagner, M. B-B Bond Nucleophilicity in a Tetraaryl m-Hydridodiborane(4) Anion. *Angew. Chem.* **2020**, *132*, 7800 –7805 (b) Kennedy, J. D. The Polyhedral Metallaboranes Part II. Metallaboranes Clusters with Eight Vertices and More. *Prog. Inorg. Chem.* **2007**, *34,* 211–434. (c) Zheng, F.; Yui, T. H.; Zhang, J.; Xie, Z. Synthesis and X-ray characterization of 15- and 16- vertex closo-carboranes. *Nat. Commun*. **2020**, *11,* 5943. (d) Stauber, J. M.; Schwan, J.; Zhang, X.; Axtell, J. C.; Jung, D.; McNicholas, B. J.; Oyala, P. H.; Martinolich, A. J.;. Winkler, J. R.; See, K. A.; Miller, III, T. F.; Gray, H. B.; Spokoyny, A. M. A Super-Oxidized Radical Cationic Icosahedral Boron Cluster. *J. Am. Chem. Soc.* **2020**, *142*, 30, 12948–12953. (e) Kar, S.; Ghosh, S. Borane Polyhedra Beyond Icosahedron. In 50th Anniversary of Electron Counting Paradigms for Polyhedral Molecules. *Struct. Bonding (Berlin)*; Mingos, D.; Ed. **2021**, *187*, 109–138. (f) Kar, S., Bairagi, S., Haridas, A., Joshi, G., Jemmis, E. D., Ghosh, S. Hexagonal Planar $[B_6H_6]$ within a $[B_6H_{12}]$ Borate Complex: Structure and Bonding of $[(Cp^*Ti)_2(\mu\text{-}\eta^6:\eta^6\text{-}B_6H_6)(\mu\text{-}H)_6]$**.** *Angew. Chem. Int. Ed.* **2022,** *61*, e202208293. (g) Ghosh, S.; Nollb B., C.; Fehlner, T. P. Expansion of iridaborane clusters by addition of monoborane. Novel metallaboranes and mechanistic detail. *Dalton Trans.* **2008**, *3*, 371–378.

(9) (a) Greenwood, N. N.; Kennedy, J. D.; Reed D. Reactions of the Octahydrotriborate(1-) Anion, $[B_3H_8]^-$, with Some Complexes of Cobalt(I), Cobalt(II), Rhodium(I), and Iridium(I), and the Characterization of the 'Borallyl' Complex $[Ir^{III}(\eta^3\text{-}B_3H_7)(CO)H(PPh_3)_2]$. *J. Chem. Soc., Dalton Trans.* **1980**, *1*, 196-200. (b) Kim, D. Y.; You, Y.; Girolami, G. S. Synthesis and crystal structures of two (cyclopentadienyl)titanium(III) hydroborate complexes: $[Cp^*TiCl(BH_4)]_2$ and $Cp_2Ti(B_3H_8)$. *J. Organomet. Chem.* **2008**, *693*, 981-986. (c) Ghosh, S.; Beatty, A. M.; Fehlner, T. P. The reaction of Cp^*ReH_6, $Cp^* = C_5Me_5$, with Monoborane to Yield a Novel Rhenaborane. Synthesis and Characterisation of arachno-$Cp^*ReH_3B_3H_8$. *Collect. Czech. Chem. Commun*. **2002**, *67*, 808-812.

(10) (a) Saha, K.; Ghorai, S.; Kar, S.; Saha, S.; Halder, R.; Raghavendra, B.; Jemmis, E. D.; Ghosh, S. Stabilization of Classical $[B_2H_5]^-$: Structure and Bonding of $[(Cp^*Ta)_2(B_2H_5)(\mu\text{-}H)L_2]$ ($Cp^* = \eta^5\text{-}C_5Me_5$; L = SCH_2S). *Angew. Chem. Int. Ed*. **2019**, *58*, 17684-17689. (b) Mondal, B.; Bag, R.; Ghorai, S.; Bakthavachalam, K.; Jemmis, E. D.; Ghosh, S. Synthesis, Structure, Bonding and Reactivity of Metal Complexes comprising Diborane(4) and Diborene(2): $[\{Cp^*Mo(CO)_2\}_2\{\mu\text{-}\eta^2\text{:}\eta^2\text{-}B_2H_4\}]$ and $[\{Cp^*M(CO)_2\}_2B_2H_2M(CO)_4]$. M=Mo,W. *Angew. Chem. Int. Ed*., **2018**, *57*, 8079. (c) Ramalakshmi, R.; Bhattacharyya, M.; Rao, C. E.; Ghosh, S. Synthesis, Structure and Chemistry of Low-Boron Containing Molybdaborane: *arachno*-$[Cp^*Mo(CO)_2B_3H_8]$. *J. Organomet. Chem.* **2015**, *792*, 31.

(11) Hoffmann, R. Building Bridges Between Inorganic and Organic Chemistry (Nobel Lecture). *Angew. Chem. Int. Ed*. *Engl*. **1982**, *21*, 711–724.

(12) (a)Fox, M. A.; Wade, K. Evolving patterns in boron cluster chemistry. *Pure Appl. Chem.* **2003**, *75*, 9, 1315–1323. (b) Mingos, D. M. P. Polyhedral skeletal electron pair approach. *Acc. Chem. Res.* **1984**, *17*, 311–319. (c) Jemmis, E. D.; Balakrishnarajan, M. M.; Pancharatna, P. D. Electronic requirements for macropolyhedral boranes. *Chem. Rev.* **2002**, *102*, 93–144.

(13) Andersen, E. L.; Haller, K. J.; Fehlner, T. P. Ferraborane $B_3H_7Fe_2(CO)_6$, a Diiron Analogue of Pentaborane(9). *J. Am. Chem. Soc.* **1979**. 4390-4391.

(14) Lei, X.; Shang, M.; Fehlner, T. P. Chemistry of Dimetallabor of Organometallic Chemistry 952 (2021) 122023anes Derived from the Reaction of $[Cp^*MCl_2]_2$ with Monoboranes (M = Ru, Rh; $Cp^* = \eta^5\text{-}C_5Me_5$). *J. Am. Chem. Soc.* **1999**, *121*, 6, 1275–1287.

(15) Gregoriades, L. J.; Zabel, M.; Bai, J.; Brunklaus, G.; Krossing, I.; Eckert, H.; Scheer, M. Self-Assemblies Based on $[Cp_2Mo_2(CO)_4(\mu,\eta^2\text{-}P_2)]$-Solid-State Structure and Dynamic Behaviour in Solution. *Chem. Eur. J*. **2008**, *14*, 282 – 295.

(16) Sazonov, P. K.; Beletskaya, I. P. Cyclopentadienylmolybdenum Tricarbonyl Complexes: $(\eta^5\text{-}C_5H_5)\text{-}Mo(CO)_3X$. In *Encyclopedia of Reagents for Organic Synthesis*; Wiley, 2013**,** Updated May 15, 2013.

(17) Handy, L. B.; Ruff, J. K.; Dah, L. F. Structural Characterization of the Dinuclear Metal Carbonyl Anions $[M_2(CO)_{10}]^{2-}$ (M = Cr, Mo) and $[Cr_2(CO)_{10}H]^-$. The Marked Stereochemical Effect of a Linearly Protonated Metal-Metal Bond. *J. Am. Chem. Soc.* **1970**, *92*, 25, 7312-7326.

(18) (a) Aldridge, S.; Shang, M.; Fehlner, T. P. Synthesis of Novel Molybdaboranes from $(\eta^5\text{-}C_5R_5)MoCl_n$ Precursors (R = H, Me; n = 1, 2, 4), *J. Am. Chem. Soc.* **1998**, *120*, 2586-2598. (b) Aldridge S.; Shang, M.; Fehlner, T. P. Origins of Unsaturation in Group 6 Metallaboranes. Synthesis, Crystal Structure, and Molecular Orbital Calculations for $(Cp^*MoCl)_2B_3H_7$ (Cp^*=Pentamethylcyclopentadienyl). *J. Am. Chem. Soc.* **1997**, *119*, 11120-11121. (c) Ghosh, S.; Lei, X.; Cahill, C. L.; Fehlner, T. P.; Symmetrical Scission of the Coordinated Tetraborane in $[(Cp^*ReH_2)_2\ B_4H_4]$ on CO Addition and Reassociation of the Coordinated Diboranes on H_2 loss. *Angew. Chem. Int. Ed.* **2000**, *39*, 2900–2902.

(19) (a) Aldridge, S.; Shang, M.; Fehlner, T. P. Directed Synthesis of Chromium and Molybdenum Metallaborane Clusters. Preparation and Characterization of $(Cp^*Cr)_2B_5H_9$, $(Cp^*Mo)_2B_5H_9$ and $(Cp^*MoCl)_2B_4H_{10}$. *J. Am. Chem. Soc.* **1997**, *119*, 2339-2340. (b) Geetharani, K.; Bose, S. K.; Pramanik, G.; Saha, T. K.; Ramkumar, V.; Ghosh, S. An Efficient Route to Group 6 and 8 Metallaborane Compounds: Synthesis of arachno-$[Cp^*Fe(CO)B_3H_8]$ and closo-$[(Cp^*M)_2B_5H_9]$ (M = Mo, W). *Eur. J. Inorg. Chem*. **2009**, 1483–1487. (c) Sahoo, S.; Reddy, K. H. K.; Dhayal, R. S.; Mobin, S. M.; Ramkumar, V.; Jemmis, E. D.; Ghosh. S. Chlorinated eleelectronic Dimetallaborane Clusters: Synthesis, Characterization, and Electronic Structures of $(\eta5\text{-}C_5Me_5W)_2B_5H_nCl_m$ (n = 7, m = 2 and n = 8, m = 1). *Inorg. Chem*. **2009**, *48*, 6509–6516. (d) Dhayal, R. S.; Sahoo, S.; Reddy, K. H. K.; Mobin, S. M.; Jemmis, E. D.; Ghosh, S. Vertex-Fused Metallaborane Clusters: Synthesis, Characterization and Electronic

Structure of [(η^5 -$C_5Me_5Mo)_3MoB_9H_{18}$. *Inorg. Chem*. **2010**, *49*, 900–904.
(20) Mondal, B.; Bag, R.; Ghosh, S. A Combined Experimental and Theoretical Investigations of Group 6 Dimetallaboranes [$(Cp^*M)_2B_4H_{10}$] (M = Mo and W). *Organometallics*. **2018,** *37*, 2419.
(21) Nishihara, Y.; Deck, K. J.; Shang, M.; Fehlner, T. P. Synthesis of Cobaltaborane Clusters from [$Cp^*CoCl]_2$ and Monoboranes. New Structures and Mechanistic Implications. *Organometallics.* **1994**, *13,* 4510-4522.
(22) Sharmila, D.; Ramalakshmi, R.; Chakrahari, K. K.; Varghese. B.; Ghosh, S. Synthesis, characterization and crystal structure analysis of cobaltaborane and cobaltaheteroborane clusters. *Dalton Trans*. **2014**, *43*, 9976–9985.
(23) Gomosta, S.; Kar, S.; Pradhan, A. N.; Bairagi, S.; Ramkumar, V.; Ghosh, S. Synthesis, Structures, and Bonding of Metal-Rich Metallaboranes Comprising Triply Bridging Borylene and Boride Moieties. *Organometallics*. **2021**, *40*, 529−538.
(24) Bauer, J.; Bertsch, S.; Dewhurst, R. D.; Ferkinghoff, K.; Hçrl, C.; Kraft, K.; Radacki, H.; Braunschweig, H. Hydridoborylene Complexes and Di-, Tri-, and Tetranuclear Borido Complexes with Hydride Ligands. *Chem. Eur. J*. **2013**, *19*, 17608 – 17612.
(25) Hui, Z.; Watanabe, T.; Tobita, H. Synthesis of Base-Stabilized Hydrido(hydroborylene)tungsten Complexes and Their Reactions with Terminal Alkynes To Give η^3 -Boraallyl Complexes. *Organometallics.* **2017,** *36*, 4816−4824.
(26) (a) Bag, R.; Kar, S.; Saha, S.; Gomosta, S.; Raghavendra, B.; Roisnel, T.; Ghosh, S. Heterometallic Triply-Bridging Bis-Borylene Complexes. *Chem Asian J*. **2020**, *15,* 780 –786. (b) Sharmila, D.; Mondal, B.; Ramalakshmi, R.; Kundu, S.; Babu Varghese, B.; Ghosh, S. First-Row Transition-Metal–Diborane and –Borylene Complexes. *Chem. Eur. J.* **2015**, *21*, 5074–5083. (c) Kar, S.; Pradhan, A. N.; Ghosh, S. Metal-rich Metallaboranes: Clusters Containing Triply and Tetra Bridging Borylene and Boride Units. *Coord. Chem. Rev.*, **2021**, *436*, 213796. (d) Bose, S. K.; Roy, D. K.; Shankhari, P.; Yuvaraj, K.; Mondal, B.; Sikder, A.; Ghosh, S. Syntheses and Characterization of New Vinyl-Borylene Complexes by the Hydroboration of Alkynes with [$(\mu_3$-BH)$(Cp^*RuCO)_2(\mu$-CO)Fe$(CO)_3$] *Chem. Eur. J.* **2013**, *19*, 2337 – 2343.
(27) (a) Dhayal, R. S.; Chakrahari, K. K. V.; Varghese, B.; Mobin, S. M.; Ghosh, S. Chemistry of Molybdaboranes: Synthesis, Structures, and Characterization of a New Class of Open-Cage Dimolybdaheteroborane Clusters. *Inorg. Chem*. **2010**, *49*, 7741–7747. (b) Chakrahari, K. K. V.; Mobin, S. M.; Ghosh, S. New Molybdaborane Clusters with a Bridged Phosphido Ligand. *J Clust Sci.* **2011**, *22*, 149–157.
(28) (a) Mondal, B.; Bhattacharya, S.; Ghosh, S. Heterometallic boride clusters of group 6 and 9 transition metals. *J. Organomet. Chem.* **2016**, *819*, 147-154. (b) Mondal, B.; Mondal, B.; Pal, K.; Varghese, B.; Ghosh, S. An electron-poor di-molybdenum triple-decker with a puckered [B_4Ru_2] bridging ring is an oblato-closo cluster. *Chem. Commun*. **2015**, *51*, 3828-3831. (c) Bose, S. K.; Geetharani, K.; Sahoo, S.; Reddy, K. H. K.; Varghese, B.; Jemmis, E. D..; Ghosh, S. Synthesis, Characterization, and Electronic Structure of New Type of Heterometallic Boride Clusters. *Inorg. Chem*. **2011**, *50*, 9414–9422.
(29) (a) Bag, R.; Prakash, R.; Saha, S.; Roisnel, T.; Ghosh, S. Triple-Decker Sandwich Complexes of Tungsten with Planar and Puckered Middle-Deck. *Inorg. Chem.* **2021**, *60*, 3524. (b) Bag, R.; Gayen, S.; Mohapatra, S.; Antharjanam, P. K. S.; Halet, J. F.; Ghosh, S. Planar triple-decker and capped octahedral clusters of group-6 transition metals. *J. Organomet. Chem*. **2021**, *952*, 122023, 1-8.
(30) (a) Dhayal, R. S.; Ramkumar, V.; Ghosh, S. Synthesis, Structure and Characterization of Dimolybdaheteroboranes. *Polyhedron*. **2011**, *30*, 2062-2066. (b) Chakrahari, K. K. V.; Thakur, A.; Mondal, B.; Dhayal, R. S.; Ramkumar, V.; Ghosh, S. A Close Packed Boron Rich 11-Vertex Molybdaborane with Novel Geometry. *J. Organomet. Chem*. **2012**, *710*, 75-79.
(31) Note that, the reaction also yielded [$(Cp^*Mo)_2B_5H_9$] and [$\{Cp^*Mo(CO)\}_2B_4H_6$] (Scheme S1) along with a few other air sensitive products which we were unable to characterize.
(32) Bag, R.; Saha, S.; Borthakur, R.; Mondal, B.; Roisnel, T.; Dorcet, V.; Halet, J. F.; Ghosh, S. Synthesis, Structures and Chemistry of the Metallaboranes of Group 4–9 with M_2B_5 Core Having a Cross Cluster M–M Bond. *Inorganics* **2019**, *7*, 27, 1-15.
(33) King, R. B.; Bisnette, M. B. Organometallic chemistry of the transition metals XXI. Some π-pentamethylcyclopentadienyl derivatives of various transition metals. *J. Organomet. Chem*. **1967**, *8*, 287-297.
(34) Murray, R. C.; Blum, L.; Liu, A. H.; Schrock, R. R. Simple Routes to Mono(η^5-pentamethylcyclopentadienyl) Complexes of Molybdenum(V) and Tungsten(V). *Organometallics.* **1985**, *4*, 953-954.
(35) Sheldrick, G. M. SHELXT –Crystal structure refinement with SHELXL. *Acta Cryst*. **2015**, *A71*, 3-8
(36) Sheldrick, G. M. SHELXT –Crystal structure refinement with SHELXL. *Acta Cryst*. **2015**, *C71*, 3-8.
(37) Dolomanov, O. V.; Bourhis, L. J.; Gildea, R. J.; Howard, J. A. K.; Puschmann, H. OLEX2: a complete structure solution, refinement and analysis program. *J. Appl. Cryst*. **2009**, *42*, 339.

Table of Contents artwork here

A rare saturated *closo* bimetallic triborane cluster, stabilized by early transition metal frameworks, has been isolated and structurally characterized. This triborane cluster containing 42 cluster valence electrons (CVE) is the newest addition to the series triborane species.